J. Biochem. 121, 231-237 (1997)

The States of Tyrosyl Residues in Thermolysin as Examined by Nitration and pH-Dependent Ionization[1]

Soo-Bok Lee, Kuniyo Inouye,[2] and Ben'ichiro Tonomura

Department of Food Science and Technology, Faculty of Agriculture, Kyoto University, Sakyo-ku, Kyoto, Kyoto 606-01

Received for publication, September 10, 1996

The states of 28 tyrosyl residues of thermolysin have been characterized by means of pH-jump studies and nitration with tetranitromethane. The ionization states of phenolic groups of the tyrosyl residues have also been estimated by spectrophotometric titration of the absorption change at 295 nm. The ionization of 16 tyrosyl residues was completed within 15 s after a pH-jump, and these residues are considered to be located on the surface of thermolysin. On the other hand, the ionization of the other 12 residues required 15 s to 10 min, suggesting the occurrence of a conformational change which leads to the exposure of the buried tyrosyl residues to the solvent. Sixteen tyrosyl residues were nitrated and categorized into three classes according to reactivity. The second-order rate constants of the respective classes of tyrosyl residues for nitration were evaluated as 3.32, 0.52, and 0.18 $M^{-1} \cdot min^{-1}$, and their apparent pK_a values were estimated to be 10.2, 11.4, and 11.8. Tyrosyl residues in the first class were considered to be located almost freely on the surface, while those in the second and third classes might be in constrained states.

Key words: metalloproteinase, nitration, pH-jump, thermolysin, tyrosine.

Thermolysin [EC 3.4.24.27] is a thermostable neutral metalloproteinase produced in the culture broth of *Bacillus thermoproteolyticus* (*1, 2*). It requires essentially one zinc ion for enzyme activity and four calcium ions for structural stability (*3-5*), and specifically catalyzes the hydrolysis of peptide bonds involving hydrophobic amino acid residues, especially at the P1′ site (*6*) [nomenclature according to Schechter and Berger (*7*)]. The amino acid sequence (*8, 9*) and refined three-dimensional structure (*10*) are available, and the kinetic mechanism of the reaction has been proposed (*11, 12*). Thermolysin has 28 tyrosyl residues per molecule, widely spread over the whole amino acid sequence (*8*). Generally, tyrosyl residues in a protein have a characteristic absorption in the ultraviolet region and can be selectively modified by tetranitromethane (TNM). TNM introduces a nitro group into the phenol ring of tyrosine, generating 3-nitrotyrosine, which causes changes in the spectrum and pK_a of the residue (*13*). Thus, nitration of tyrosyl residues can be used to probe the microenvironment of the residues (*13, 14*).

We have reported remarkable activation of thermolysin by high concentrations (*1-5*) of neutral salts in the hydrolysis and synthesis of *N*-carbobenzoxy-L-aspartyl-L-phenylalanine methyl ester (ZAPM), a precursor of a synthetic sweetener, as well as in the hydrolysis of FA-dipeptide amides with different amino acids at the scissile bond (*15-17*). The activation is dependent on the species of salt, and is brought about most effectively by NaCl and NaBr. The activity increases apparently in an exponential fashion with increasing salt concentration, and the activation is due entirely to an increase in the molecular activity, k_{cat}. Interestingly, the degree of activation is not dependent on the hydrophobicity of the amino acids at the scissile bond of the substrates. We have previously observed a characteristic absorption difference spectrum on mixing thermolysin with NaCl and NaBr, suggesting a conformational change of the enzyme upon interaction with the salts (*15, 18*). The activation may correlate with the difference spectrum.

The cause of the salt activation of thermolysin is currently not known. It has been suggested in the cases of some enzymes active in high salt concentrations that the salt-dependent behavior is related to their electrostatic properties (*19-21*). It is therefore of interest to investigate whether the characteristics of the surface of thermolysin are involved in the cause of the activation. In the present paper, we explore the structural features and surface properties of thermolysin in solution by examining the changes in state of the tyrosyl residues upon nitration and pH-dependent ionization.

EXPERIMENTAL PROCEDURES

Materials—A three-times crystallized and lyophilized preparation of thermolysin (Lot T8BA51; 8360 proteinase

[1] This study was supported in part (K.I.) by Grants-in-Aid for Scientific Research (nos. 05660091 and 07660109) from the Ministry of Education, Science, Sports and Culture of Japan and grants (nos. 9330 and 9652) from the Salt Science Research Foundation, Tokyo of Japan.

[2] To whom correspondence should be addressed. Tel: +81-75-753-6266, Fax: +81-75-753-6265, E-mail: inouye@kais.kais.kyoto-u.ac.jp

Abbreviations: AcTyrOEt, *N*-acetyl-L-tyrosine ethyl ester; FA, 3-(2-furyl)acryloyl; FAGLA, *N*-[3-(2-furyl)acryloyl]glycyl-L-leucine amide; GdnHCl, guanidinium hydrochloride; TLN, thermolysin; TNM, tetranitromethane; ZAPM, *N*-carbobenzoxy-L-aspartyl-L-phenylalanine methyl ester.

units/mg according to the supplier) was purchased from Daiwa Kasei, Osaka. This preparation was used without further purification. The thermolysin solution was filtered with a Millipore membrane filter, Type HA (pore size 0.45 μm), before use. The concentration was determined spectrophotometrically using an absorbance value A (1 mg/ml) at 277 nm of 1.83 (*15*) and a molecular mass of 34.6 kDa (*8*). All other reagents were of reagent grade, purchased from Nacalai Tesque (Kyoto).

Ultraviolet (UV) Difference Absorption Spectra—UV difference absorption spectra observed on the mixing of thermolysin with various alkaline solutions were measured with a Shimadzu UV-2200 spectrophotometer at 25°C. Two sets of quartz cells in tandem with a 1-cm light path were used (*14, 18*). Difference spectra were measured at 3 h after mixing thermolysin with the alkaline solutions at 25°C. The final concentration of thermolysin was 3.9 μM.

pH-Jump—Equal volumes of aqueous unbuffered thermolysin solution and NaOH of various concentrations were mixed to induce a pH-jump at 25°C (*22, 23*). The standardization of NaOH solution was performed by using oxalic acid. The absorption change induced by the pH-jump was followed at 245 nm with a Shimadzu UV-2200 spectrophotometer. The final pH of the solution was determined in the pH range below pH 12.5 by a Hitachi-Horiba F-5 pH meter, and estimated by calculation in the pH range above pH 12. The concentration of *N*-acetyl-L-tyrosine ethyl ester (AcTyrOEt) was determined spectrophotometrically using the molar absorption coefficient $\varepsilon_{274.5}=1.34\times10^3$ $M^{-1}\cdot cm^{-1}$ at 25°C (*14*). The number of ionized tyrosyl residues was determined from the molar absorption difference obtained for the ionization of AcTyrOEt, $\Delta\varepsilon_{245}=11.0\times10^3$ $M^{-1}\cdot cm^{-1}$ and $\Delta\varepsilon_{295}=2.33\times10^3$ $M^{-1}\cdot cm^{-1}$ (*14*). The apparent first-order rate constant, k_{app} for the absorption curve induced by the pH-jump was estimated from a Guggenheim plot (*24*).

Spectrophotometric Titration of Tyrosyl Residues—The titration of phenolic hydroxyl groups of tyrosyl residues in thermolysin was performed spectrophotometrically by measuring the absorptivity difference at 295 nm between the alkaline and neutral solutions at pH 7.0. Forty millimolar glycine-NaOH buffer was used for the entire pH range employed. NaCl was added to maintain the ionic strength of solutions at 0.2 M. The final concentration of protein used for the titration was 1.85 μM. The optical measurement was made within 10 min after the preparation of the alkaline sample.

For the titration in the presence of GdnHCl, 0.2 ml of a thermolysin solution at pH 7.0 was mixed with 2 ml of a mixture of 0.5 N NaOH and 0.5 M NaCl containing 4.2 M guanidinium hydrochloride (GdnHCl), giving the desired pH values. The mixture was allowed to stand for 30 min at 25°C before spectrophotometric measurements. The final protein concentration was 3.5 μM. Molar absorptivity difference at 295 nm between the alkaline and neutral solutions is considered to be unaffected by the presence of 3.8 M GdnHCl (*14*).

Evaluation of Data for Spectrophotometric Titration—The titration data in a given pH range were evaluated stepwise by fitting to a theoretical ionization curve based on the following equation,

$$\Delta\varepsilon=\Delta\varepsilon_{max}/(1+[H^+]/K) \quad (1)$$

where $\Delta\varepsilon_{max}$ is the molar absorptivity difference after complete ionization of all tyrosines, K is the apparent ionization constant, and $\Delta\varepsilon$ is the molar absorptivity difference at a given pH value. Direct curve-fitting was performed using a home-made program to obtain the $\Delta\varepsilon_{max}$ value and the apparent K value, K_{app}. The iterative curve-fitting was carried out stepwise so that the deviation between the raw data and the theoretical equation in a confined region was minimized. The number of ionized tyrosyl residues in the protein was calculated from the $\Delta\varepsilon_{max}$ value using a value for $\Delta\varepsilon_{295}$ of 2.33×10^3 $M^{-1}\cdot cm^{-1}$ for the ionization of a single phenolic group (*14*).

Nitration of AcTyrOEt—AcTyrOEt (0.11 mM) was mixed with an 80-fold molar excess of TNM in 40 mM Tris-HCl buffer (pH 8.0) containing 10 mM $CaCl_2$ at 25°C. The reaction was followed spectrophotometrically by measuring the increase in absorbance at 350 nm due to the formation of *N*-acetyl-3-nitrotyrosine ethyl ester (*13*). The increase in absorbance due to degradation of TNM in the alkaline buffer was subtracted as a blank from the reaction curve monitored by using a double tandem cell system (*14*). The concentration of *N*-acetyl-3-nitrotyrosine ethyl ester produced was determined spectrophotometrically using the molar absorption coefficient of nitroformate [$C(NO_2)_3^-$], $\varepsilon_{350}=14.4\times10^3$ $M^{-1}\cdot cm^{-1}$, on the assumption that the increase in absorbance corresponds to the formation of 1 mol of nitroformate/mol of AcTyrOEt (*13*).

Nitration of Thermolysin—Nitration of thermolysin was performed by adding an appropriate portion of 1 or 10% solution of TNM in methanol to the protein solution (7–9 μM) in 40 mM Tris-HCl buffer containing 10 mM $CaCl_2$, pH 8.0. The reaction mixture was maintained at 25°C for a suitable period of time and the reaction was terminated by gel-filtration on a Bio-Gel P-4 column [1.5 cm (diameter) × 25 cm] equilibrated with the same buffer. The degree of nitration was determined from the absorbance at 381 nm (a nitrophenol-nitrophenolate isosbestic point of 3-nitro-L-tyrosine), using the molar absorption coefficient of 2.2×10^3 $M^{-1}\cdot cm^{-1}$ (*13, 25*). The concentration of nitrated thermolysin was determined by measuring the absorbance of the protein preparation at 275 nm, pH 8.0 by using the molar absorption coefficient for native thermolysin, $\varepsilon_{275}=62.25\times10^3$ $M^{-1}\cdot cm^{-1}$, according to the procedures described previously (*15, 26*).

RESULTS

Time-Dependence of Phenolic Ionization by pH-Jump—Difference spectra of thermolysin in alkaline solution were observed against the solution at pH 7.0 (Fig. 1). The difference spectra show maxima around 245 and 295 nm, indicating the ionization of phenolic hydroxyl groups of tyrosyl residues. The number of ionizable tyrosyl residues at pH 13.1 was calculated to be 27.8, being in good agreement with the result of amino acid analysis, 28. Figure 2 shows time courses of the change in absorption difference at 245 nm (ΔA_{245}) due to mixing thermolysin with alkaline solutions. No change could be detected within 15 s after pH-jump. The contribution of ionization of sulfhydryl groups to the change does not need to be considered because

thermolysin has no cysteine residues. No time-dependent change was observed below pH 12.1, although the total change increased with increasing pH value. Above pH 12.1, however, a time-dependent change was observed. The rate of the change increased as the pH was increased, and the time-dependent change was completed within 15 s at pH 12.6. The number of tyrosyl residues involved in the time-dependent ionization was estimated to be 12 from the changes in the absorption difference at 10 min observed at pH above 12.1, and their pK_a value was supposed to be above 12.2. The apparent first-order rate constants, k_{app}s were determined for the time-dependent curves: 1.9×10^{-3} s^{-1} at pH 12.2, 2.1×10^{-3} s^{-1} at pH 12.25, 6.2×10^{-3} s^{-1} at pH 12.3, 21×10^{-3} s^{-1} at pH 12.4, and 89×10^{-3} s^{-1} at pH 12.5. Figure 3 shows the pH-dependence of log k_{app}, where the slope reflects the number of tyrosyl residues cooperatively involved in the conformational changes (*22, 23*). The slope was evaluated to be 5.94 ± 0.05, suggesting that 6 tyrosyl residues buried in the native enzyme were cooperatively exposed to the water medium.

Spectrophotometric Titration of Phenolic Hydroxyl Groups—Molar absorption difference at 295 nm between neutral and alkaline solutions of thermolysin is plotted against pH (Fig. 4). Curve A represents the ionization of the tyrosyl phenolic groups measured within 10 min after the preparation of the alkaline sample. Curve D shows the phenolic hydroxyl ionization in the presence of 3.8 M GdnHCl 30 min after the mixing of the enzyme and alkaline buffer at 25°C. From the fitting analysis, there appeared to be three stages of ionization, as shown in Fig. 4. Fitting to curve A was performed in the range of pH 9–10.5 with a correlation coefficient of 94.4%, and yielded a theoretical curve A′ for 7.4 phenolic groups with pK_a 10.2. Subtraction of curve A′ from the experimental points of curve A gave curve B, to which the second fitting was successively carried out up to pH 11.6, and a theoretical curve B′ was obtained for 6.2 groups with pK_a 11.4 with a correlation of 89.2%. The third fitting to curve C given by subtracting curve B′ from curve B was finally performed up to pH 12.1 with a

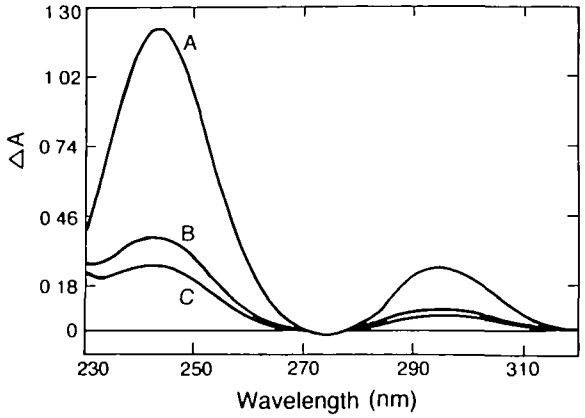

Fig. 1. **pH-difference spectra of thermolysin at alkaline pH.** A: pH 13.1. B: pH 11.2. C: pH 10.5. The pH of thermolysin solution in the reference cell was 7.0. The thermolysin concentration was 3.9 μM in a mixture of 1 M NaOH and 1 M NaCl (A), and in 40 mM glycine-NaOH buffer containing 0.2 M NaCl (B and C), at 25°C.

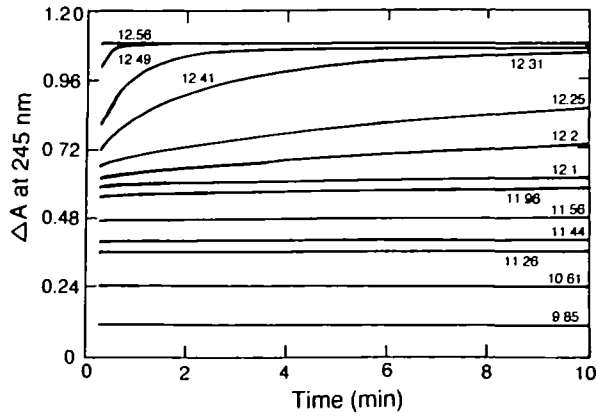

Fig. 2. **Time courses of absorption change of thermolysin at 245 nm upon pH-jump-up.** An aqueous solution of thermolysin was mixed with NaOH solution at 25°C. The final enzyme concentration was 3.5 μM. The figures indicated are the final pH after pH-jump-up. The absorption change within 15 s after the pH-jump could not be recorded.

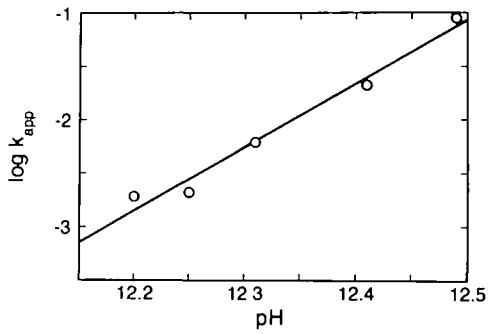

Fig. 3. **pH dependence of the apparent first-order rate constant, k_{app}, for the time-dependent phase in the absorbance change of thermolysin after pH-jump.** The apparent first-order rate constants were obtained from Guggenheim plots.

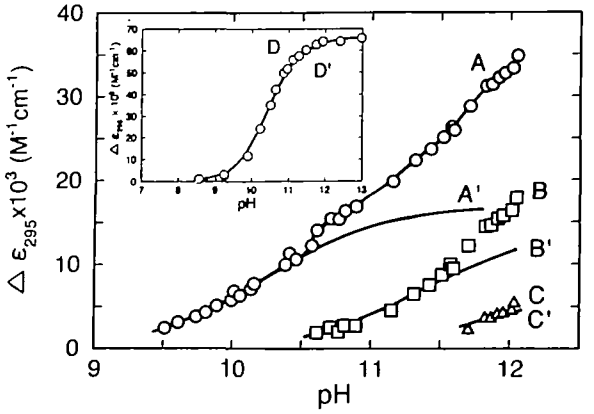

Fig. 4. **Spectrophotometric titration curves of thermolysin.** A (○): Titration curve. The concentration of thermolysin was 1.85 μM. A′: A theoretical ionization curve for 7.4 tyrosyl residues with pK_a 10.2. B (□): Difference between experimental values of A and theoretical values of A′. B′: A theoretical ionization curve for 6.2 tyrosyl residues with pK_a 11.4. C (△): Difference between B and B′. C′: A theoretical ionization curve for 3.2 tyrosyl residues with pK_a 11.8. D (○) in inset: Titration in the presence of 3.8 M GdnHCl. The line is a theoretical curve for 28 tyrosyl residues with pK_a 10.4.

correlation of 91.9%, and a theoretical curve C′ was obtained for 3.2 groups with pK_a 11.8. Curve D was fitted to a theoretical ionization curve for 28.0±0.3 phenolic groups with pK_a 10.4±0.1.

Reactivity of Tyrosyl Residues with TNM—As shown in Fig. 5, the reaction of AcTyrOEt with TNM followed simple pseudo-first-order kinetics represented by the following equation.

$$\ln\{([NO_2\text{-AcTyrOEt}]_{total} - [NO_2\text{-AcTyrOEt}]_t)/[NO_2\text{-AcTyrOEt}]_{total}\} = -k_{app} \cdot t \quad (2)$$

$[NO_2\text{-AcTyrOEt}]_{total}$ represents the total concentration of nitrated AcTyrOEt at time ∞, and is equal to the initial concentration of AcTyrOEt. $[NO_2\text{-AcTyrOEt}]_t$ is the concentration of nitrated AcTyrOEt at a given time, t. The apparent first-order rate constant, k_{app}, was evaluated to be $16.7(\pm0.2)\times10^{-3}$ min^{-1} from the slope of the straight line by the least-squares method. Since the initial concentration of TNM was 8.4 mM, the second-order rate constant for the nitration of AcTyrOEt was calculated to be 1.99(±0.02) M^{-1}·min^{-1}. It is noteworthy that there is a slight discrepancy between the formation of the nitrated AcTyrOEt (open circles) and the theoretical curve expressing a pseudo-first-order reaction (solid line) in the time range of 0-40 min (Fig. 5). Self-association of AcTyrOEt could be the cause of this phenomenon.

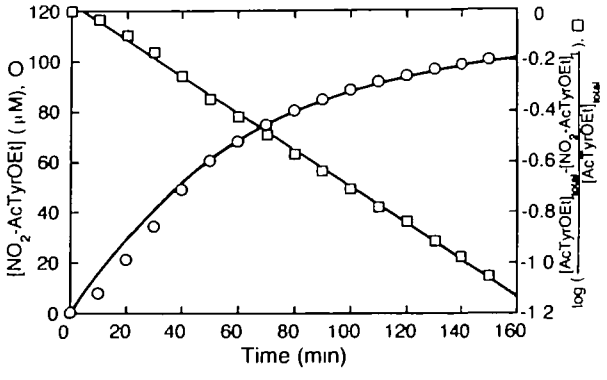

Fig. 5. **Time course of the nitration of AcTyrOEt with TNM.** The nitration was carried out with 80-fold molar excess of TNM in 40 mM Tris-HCl buffer at pH 8.0, 25°C. The molar concentration of nitrated AcTyrOEt is shown by open circles, and the pseudo-first-order plot, by open squares. The line drawn on the open circles represents a theoretical curve.

Figure 6A shows the progress of nitration as a function of the molar ratio of TNM to thermolysin, [TNM]/[TLN], ranging from 20 to 1,930 in 40 mM Tris-HCl buffer containing 10 mM $CaCl_2$, pH 8.0. [TLN] indicates initial concentration of native thermolysin in the reaction mixture. The degree of nitration increased with increasing ratio, and reached the level corresponding to 9 nitrotyrosyl residues per molecule at [TNM]/[TLN] of 1,930. Nitration proceeded as a function of time in a range of 0 to 15 h at 25°C at [TNM]/[TLN] of 2,000 (Fig. 6B), and reached the saturation level, corresponding to 16 nitrotyrosyl residues per molecule, within 15 h. When the molar ratio of [TNM]/[TLN] was 2,000, the molar ratio of TNM to tyrosyl residue to be nitrated in thermolysin, [TNM]/[TYR], for the nitrated thermolysin was calculated to be 125. Since [TNM] ≫ [TYR], nitration of thermolysin was

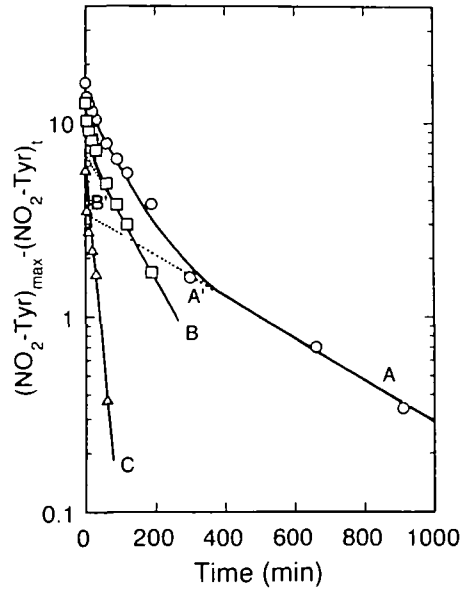

Fig. 7. **Analysis of the reaction of 7 μM thermolysin with 14 mM TNM by means of a semi-logarithmic plot.** The analysis was carried out as described in "EXPERIMENTAL PROCEDURES." A (○): original curve, which represents the difference between the numbers of tyrosyl residues nitrated maximally $[(NO_2\text{-Tyr})_{max}]$, 16, and of tyrosyl residues nitrated at a given time $[(NO_2\text{-Tyr})_t]$. A′ (·····): extrapolated portion of the final slope of the original curve. B (□): difference values of the original and extrapolated curve. B′ (·····): extrapolated portion of the final slope of curve B. C (△): difference values of curves B and B′.

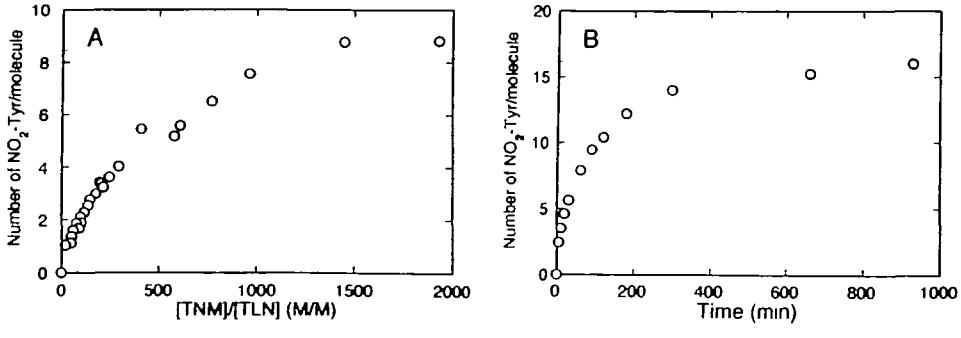

Fig. 6. **(A) Nitration of thermolysin with TNM.** The reaction was carried out by adding an appropriate volume of 1% methanolic TNM solution in 40 mM Tris-HCl buffer (pH 8.0) containing 10 mM $CaCl_2$ for 1 h at 25°C. The initial concentrations of native thermolysin in mixed solution were 8.0-8.7 μM. **(B) Time course of the nitration of thermolysin.** The initial concentrations of native thermolysin and TNM in mixed solution were 7 μM and 14 mM, respectively. The reaction was carried out under the same conditions as above.

TABLE I. **The states of the tyrosyl residues of thermolysin.**

pH jump		pH titration			Nitration	
	No.	Class	pK_a	No.	k ($M^{-1}\cdot min^{-1}$)	No.
Ionizable		I	10.2	7.4	3.32	5.8
at pH 12.1	16	II	11.4	6.2	0.52	6.9
within 15 s		III	11.8	3.2	0.18	3.4
Ionizable at pH 12.2-12.6 in 15 s-10 min	6		–	–	–	–
Not-ionizable at pH 12.6 in 10 min	6		–	–	–	–

assumed to follow pseudo-first-order kinetics. However, the reaction did not give a simple pseudo-first-order curve (Fig. 7). On the assumption that several classes of reacting tyrosyl residues exist, each having a specific reaction rate constant, the following equation for the second-order reaction can be written:

$$-k_i \cdot t = 1/[\mathrm{TNM}] \cdot \ln(1 - n_i/N_i) \quad (3)$$

where [TNM] is the molar concentration of TNM, n_i is the number of nitrated tyrosyl residues of the ith class at time t, N_i is the maximal number of nitrated tyrosyl residues of the ith class when the reaction has proceeded to completion, and k_i is the second-order rate constant for the ith class. Equation 3 is converted to

$$n_i = N_i \cdot (1 - \exp(-k_i \cdot [\mathrm{TNM}] \cdot t)) \quad (4)$$

If the three reactions occur simultaneously, the following equation is derived for the slowest reaction, *i.e.* the third one ($i=3$).

$$-k_3 \cdot t = 1/[\mathrm{TNM}] \cdot (\ln(N_{max} - n) - \ln N_3) \quad (5)$$

where N_{max} and n are the maximal number of nitrated tyrosyl residues and the number at time t, respectively. Since N_{max} corresponds to 16 and [TNM] is 1.4×10^{-3} M in the present experiment, Eq. 5 gives

$$\ln(16 - n) = -0.014 \cdot k_3 \cdot t + \ln N_3 \quad (6)$$

The straight line based on Eq. 6 was first fitted to the original reaction curve A. The values of $\ln(16-n)$ in the extrapolated line A′ were subtracted from the corresponding values in the original curve A. These difference values were plotted semi-logarithmically and gave curve B. Since curve B deviated from a straight line, B′, the previous procedure was repeated. The second set of difference values giving curve C was made to fit a straight line. From the best-fit straight lines representing component pseudo-first-order reactions in Fig. 7, the second-order rate constant and the number of each class of tyrosyl residues were determined, respectively, to be $k_1 = 3.32\ M^{-1}\cdot min^{-1}$ and $N_1 = 5.8$ for the first class, $k_2 = 0.52\ M^{-1}\cdot min^{-1}$ and $N_2 = 6.9$ for the second class, and $k_3 = 0.18\ M^{-1}\cdot min^{-1}$ and $N_3 = 3.4$ for the third class.

The results on the states of the 28 total tyrosyl residues of thermolysin are summarized in Table I. The pH-jump experiment suggests that 16 tyrosyl residues are located on the surface of thermolysin. The pH-dependent ionization and nitration indicate that 16 residues can be classified into 3 independent groups. These results are in good accord with each other, and suggest that the 16 residues are accessible to the solvent and can be classified according to their ionizability and reactivity to nitration. The most reactive 6-7 residues are in class I, another 6-7 are in class II, and the other 3 are in class III. The 12 buried residues are classified into two groups; 6 are ionized during incubation at pH 12.2-12.6 for 15 s-10 min, and the other 6 are not ionized during incubation at pH 12.6 for 10 min.

DISCUSSION

Conformational Changes Due to pH-Jump—Tyrosyl residues of enzymes have characteristic spectrophotometric properties due to ionization and have been used as probes in conformational studies of proteins (*22, 23, 27*). In the present study, we focused primarily on investigating the states of tyrosyl residues of thermolysin in solution. A pH-jump method which is based on spectrophotometric changes with time in the alkaline region was used to observe the ionization of the tyrosyl residues. This observation allowed us to separate two phases of ionization. One was time-independent and the other, time-dependent. The time-dependent phase of ionization observed above pH 12.1 is considered to be attributable to a conformational change, resulting in exposure to the solvent of tyrosyl residues that were originally buried in the native structure. These results are consistent with our unpublished observation that thermolysin which had been incubated at pH 4-12 for 30 min showed full activity in the hydrolysis of *N*-[3-(2-furyl)acryloyl]glycyl-L-leucine amide in 40 mM Tris-HCl buffer, pH 7.5, and that autolysis was not detected during incubation at pH 6-12 for 2 h (Lee, S.-B., unpublished observations). The CD spectrum of thermolysin at pH 12 is almost the same as that at neutral pH (Kuzuya, K. and Inouye, K., unpublished observations), suggesting that the conformation of the enzyme is not much changed in the pH range from 7 to 12.

Ionization of tyrosyl residues exposed to the solvent is in general too fast to be detected with a conventional spectrophotometer and thus the time-dependent change in absorption reflects the change in the environmental state of tyrosyl residues. The number of tyrosyl residues involved in the exposure due to the conformational change was evaluated to be about 12. At the final stage of the denaturation process of thermolysin with 3.8 M GdnHCl, 28 tyrosyl residues were detected. This suggests complete unfolding of the enzyme in the denaturation process. Tyr-83 and Tyr-84 are considered to exist in the internal α-helix of thermolysin (*10*). The plot of log k_{app} *vs.* pH in Fig. 3 gives a straight line with a slope of about 6. This value is noticeably larger than that for pepsin (0.5) and corresponds approximately to the mean value of the slopes for bacterial α-amylase (1.0-11.5) (*22, 23*). The time-independent phase of ionization in Fig. 2 does not show whether or not the tyrosyl residues in this phase are totally exposed to the solvent in the intact state, since conformational changes, if they occur, within the dead time (15 s) can not be observed in the present detection method. In order to examine this point, nitration of tyrosyl residues on the surface of thermolysin with TNM was performed.

Classification of Tyrosyl Residues by Reactivity with TNM—In the reaction of thermolysin with TNM, which reacts with exposed tyrosyl residues, tyrosyl residues in the time-independent phase (Fig. 2) could be nitrated as

shown in Fig. 6B. Thus, 16 out of 28 total tyrosyl residues of thermolysin are exposed on the surface in solution and can react with TNM. This result indicates that the tyrosyl residues in thermolysin tend to exist on the surface as well as in the interior; this tendency has been observed in subtilisins as well (*28*). The surface tyrosyl residues in thermolysin are individually situated in different electrostatic and hydrophobic microenvironments and are classified into three groups of ionization state. These surface tyrosyl residues can be categorized according to their reactivity with TNM, which is dependent on the ionization state of the residues. The surface tyrosyl residues are also expected to follow first-order kinetics for nitration, when the exposed residues are nitrated independently, as suggested for trypsinogen in the previous report (*29*). The surface tyrosyl residues of thermolysin were divided into three classes (Fig. 7). The second-order rate constant (3.32 $M^{-1}\cdot min^{-1}$) of the first class of 6 tyrosyl residues is slightly lower than that (6.0 and 6.7 $M^{-1}\cdot min^{-1}$) for trypsin and trypsinogen (*29*). The second (7 tyrosyl residues) and third (3 tyrosyl residues) classes, accounting for 10 out of 16 residues exposed on the surface, show rather low reactivity, corresponding to 17% (0.52 $M^{-1}\cdot min^{-1}$) and 7% (0.18 $M^{-1}\cdot min^{-1}$) of the rate constant of the first class, respectively. This fact suggests that the microenvironments of the second and third classes of tyrosyl residues are negatively charged and/or hydrophobic. The pK_a value, 10.2 of the first class of tyrosyl residues is slightly higher than that (pK_a 9.7) observed with *Streptomyces* subtilisin inhibitor and subtilisin BPN′. This pK_a value, together with the lower rate constant of the first class for nitration, suggests that tyrosyl residues in the first class of thermolysin are not entirely free on the surface, but are slightly constrained. The higher pK_a values, 11.4 and 11.8, of the second and the third classes may reflect microenvironments unfavorable to ionization. The states of tyrosyl residues on the surface of thermolysin were estimated on the basis of an X-ray crystallographic analysis (*10*). Five residues (Tyr-75, 110, 211, 251, and 296) are within 3-7 Å of positively charged groups and are expected to ionize more easily than the others. The accessibility to water of Tyr-24 and 27 is higher than 90%, and no negatively charged residues are present around them. Accordingly, they might be in the first class. Tyr-66, 193, 217, and 274 are close to negatively charged groups (within 3-5 Å), and their ionization is considered to be fairly suppressed. They might be candidates for the third class. Thus, the remaining residues such as Tyr-46, 151, 157, 179, 221, and 242, whose accessibility to water was calculated to be 40%, might belong to the second class.

Identification of the nitrated tyrosyl residues and the effect of nitration on the salt-activation of thermolysin are in progress. Recently, we found that the degree of activation of thermolysin by the addition of NaCl decreased with increasing degree of nitration of tyrosyl residues, whereas the degree of activation recovered to the level of native thermolysin when the nitrated tyrosyl residues were aminated (Lee, S.-B. and Inouye, K., unpublished observations). These observations suggest that the ionization states of the tyrosyl residues of thermolysin are closely related to the halophilic properties of this enzyme.

REFERENCES

1. Endo, S. (1962) Studies on protease produced by thermophilic bacteria (in Japanese) *J. Ferment. Technol.* **40**, 346-353
2. Matsubara, H. and Feder, J. (1971) Other bacterial, mold, and yeast proteases in *The Enzymes* 3rd ed. (Boyer, P.D., ed.) Vol. 3, pp. 721-795, Academic Press, New York
3. Latt, S.A., Holmquist, B., and Vallee, B.L. (1969) Thermolysin: A zinc metalloenzyme. *Biochem. Biophys. Res. Commun.* **37**, 333-339
4. Feder, J., Garrett, L.R., and Wildi, B.S. (1971) Studies on the role of calcium in thermolysin. *Biochemistry* **10**, 4552-4555
5. Tajima, M., Urabe, I., Yutani, K., and Okada, H. (1976) Role of calcium ions in the thermostability of thermolysin and *Bacillus subtilis* var. *amylosaccharitícus* neutral protease. *Eur. J. Biochem.* **64**, 243-247
6. Morihara, K. and Tsuzuki, H. (1970) Thermolysin: Kinetic study with oligopeptides. *Eur. J. Biochem.* **15**, 374-380
7. Schechter, I. and Berger, A. (1967) On the size of the active site in proteases. I. Papain. *Biochem. Biophys. Res. Commun.* **27**, 157-162
8. Titani, K., Hermodson, M.A., Ericsson, L.H., Walsh, K.A., and Neurath, H. (1972) Amino-acid sequence of thermolysin. *Nature* **238**, 35-37
9. O'Donohue, M.J., Roques, B.P., and Beaumont, A. (1994) Cloning and expression in *Bacillus subtilis* of the *npr* gene from *Bacillus thermoproteolyticus* Rokko coding for the thermostable metalloprotease thermolysin. *Biochem. J.* **300**, 599-603
10. Holmes, M.A. and Matthews, B.W. (1982) Structure of thermolysin refined at 1.6 Å resolution. *J. Mol. Biol.* **160**, 623-639
11. Hangauer, D.G., Monzingo, A.F., and Matthews, B.W. (1984) An interactive computer graphics study of thermolysin-catalyzed peptide cleavage and inhibition by *N*-carboxymethyl dipeptides. *Biochemistry* **23**, 5730-5741
12. Mock, W.L. and Aksamawati, M. (1994) Binding to thermolysin of phenolate-containing inhibitors necessitates a revised mechanism of catalysis. *Biochem. J.* **302**, 57-68
13. Sokolovsky, M., Riordan, J.F., and Vallee, B.L. (1966) Tetranitromethane. A reagent for the nitration of tyrosyl residues in proteins. *Biochemistry* **5**, 3582-3589
14. Inouye, K., Tonomura, B., Hiromi, K., Sato, S., and Murao, S. (1977) The states of tyrosyl and tryptophyl residues in a protein proteinase inhibitor (*Streptomyces* subtilisin inhibitor). *J. Biochem.* **82**, 1207-1215
15. Inouye, K. (1992) Effects of salts on thermolysin: Activation of hydrolysis and synthesis of *N*-carbobenzoxy-L-phenylalanine methyl ester, and a unique change in the absorption spectrum of thermolysin. *J. Biochem.* **112**, 335-340
16. Inouye, K., Lee, S.-B., and Tonomura, B. (1996) Effect of amino acid residues at the cleavable site of substrates on the remarkable activation of thermolysin by salts. *Biochem. J.* **315**, 133-138
17. Inouye, K. (1994) Halophilic enzymes (in Japanese). *Seikagaku* **66**, 446-450
18. Inouye, K., Kuzuya, K., and Tonomura, B. (1994) A spectrophotometric study on the interaction of thermolysin with chloride and bromide ions, and the state of tryptophyl residue 115. *J. Biochem.* **116**, 530-535
19. Zaccai, G. and Eisenberg, H. (1990) Halophilic proteins and the influence of solvent on protein stabilization. *TIBS* **15**, 333-337
20. Madern, D., Pfister, C., and Zaccai, G. (1995) Mutation at a single acidic amino acid enhances the halophilic behaviour of malate dehydrogenase from *Haloarcula marismortui* in physiological salts. *Eur. J. Biochem.* **230**, 1088-1095
21. Szeltner, Z. and Polgár, L. (1996) Conformational stability and catalytic activity of HIV-1 protease are both enhanced at high salt concentration. *J. Biol. Chem.* **271**, 5458-5463
22. Hiromi, K., Ohnishi, M., Kanaya, K., and Matsumoto, T. (1975) The pH jump study of enzyme proteins. I. Liquefying α-amylase from *Bacillus subtilis*. *J. Biochem.* **77**, 957-963
23. Kitagishi, K. and Hiromi, K. (1986) pH-jump of pepsin studied by tyrosine ionization. *Agric. Biol. Chem.* **50**, 1113-1116

24. Guggenheim, E.A. (1926) On the determination of the velocity constant of a unimolecular reaction. *Phil. Mag.* **2**, 538-543
25. Inouye, K., Tonomura, B., and Hiromi, K. (1979) The interaction of a tyrosyl residue and carboxyl groups in the specific interaction between *Streptomyces* subtilisin inhibitor and subtilisin BPN'. A chemical modification study. *J. Biochem.* **85**, 1115-1126
26. Goto, K., Takahashi, N., and Murachi, T. (1971) Chemical modification of tyrosyl residues of stem bromelain. *J. Biochem.* **70**, 157-164
27. Donovan, J.W. (1973) Spectrophotometric titration of the functional groups of proteins. *Methods Enzymol.* **27**, 525-548
28. Myers, B., II and Glazer, A.N. (1971) Spectroscopic studies of the exposure of tyrosine residues in proteins with special reference to the subtilisins. *J. Biol. Chem.* **246**, 412-419
29. Vincent, J.P., Lazdunski, M., and Delaage, M. (1970) On the use of tetranitromethane as a nitration reagent. The reaction of phenol side-chains in bovine and porcine trypsinogens and trypsins. *Eur. J. Biochem.* **12**, 250-257